How Can Computer Simulations Contribute to Understand the Static Structure of Glasses? *

Kurt Binder and Walter Kob

Institut für Physik, Johannes-Gutenberg-Universität Mainz

D-55099 Mainz, Staudinger Weg 7, Germany

November 30, 1997

Introduction: The Molecular Dynamics Method

Many different computational techniques are denoted as "computer simulation", from "macroscopic" techniques, such as finite element methods to calculate mechanical properties, to "microscopic" techniques that deal with nuclei and electrons to calculate the electronic structure of materials (e.g., the density functional method [1]). However, in the present article we mean by *structure* the geometric arrangement of atoms considering typical length scales from 0.2 Å to 20 Å. In particular, we are interested in how this geometric structure depends on the chemical constituents (SiO_2, B_2O_3, ...), thermodynamic variables (temperature T, pressure p), cooling history by which the glass was prepared, etc. As input to such a simulation on the atomistic scale, one wishes to take a suitable *force field* that describes the interaction between the atoms, treating them like *point particles in classical mechanics*. Of course, this neglect of all quantum effects is a severe limitation of the approach that we are going to describe, and in principle it can be avoided by more accurate methods: the Car-Parrinello method [2] combines molecular dynamics

*To appear in *Analysis of Composition and Structure of Glass, and Glass Ceramics* Eds.: H. Bach and D. Krause (Springer, Berlin, 1998)

with the density functional treatment of electronic structure which depends properly on the coordinates of the nuclei, and thus avoids the approximations inherent in the force field to some extent — the path integral Monte Carlo method [3] takes into account the Heisenberg uncertainty principle (i.e., the fact that one cannot specify precisely simultaneously positions and momenta of the nuclei, since the latter are spread out over a region of the order of the de Broglie wavelength), and thus allows a correct treatment of the thermal properties of solids at low temperatures.

Although the application of either technique to materials like SiO_2 may yield promising results in the near future, we confine ourselves here to the molecular dynamics (MD) methods in the framework of classical statistical mechanics [4]. Unlike the techniques proposed more recently [2,3], applications of MD to simulate glasses have been developed since a long time [5], and we feel that recent applications [6,7] allow a rather precise and detailed description of both the structure and the thermal properties of glasses.

Basically, the MD simulation tries to mimic the experimental procedure by which a glass is produced from the melt that is cooled down sufficiently fast to bypass crystallization. However, as will be discussed below, an important difference between experiments and simulations is that in the MD method cooling rates are many orders of magnitude faster than in reality, and these extremely fast cooling schedules do have an effect on the physical properties of the "glass" observable in such a "computer experiment" [6]. To bypass this difficulty, there are actually many attempts to directly create the amorphous structure of silica glass or other so-called "continuous random networks" by direct construction [8]. For example, one uses topological rules (e.g. in amorphous SiO_2 each silicon atom has to have four oxygen atoms as neighbors, each oxygen atom has to have two silicon atoms as neighbors, the length of the covalent Si–O-bond is taken as constant and used as an input parameter) but allows for some disorder (e.g. the angles between covalent bonds are taken from some ad-hoc chosen distributions which are often optimized to match the experimental radial pair distribution function [8]). We feel, however, that despite its successes to reproduce certain known facts about the geometrical structure of glasses this heuristic approach suffers from unknown (and hence uncontrolled)

errors, unlike MD which — in the framework of classical statistical mechanics — is a "first principles"-method. We also mention that an alternative "first principles"-method is Monte Carlo sampling [9]. There one generates configurations of the model system distributed according to the canonical distribution function of statistical mechanics, i.e. proportional to $\exp(-\mathcal{H}/k_BT)$ where $\mathcal{H}$ is the Hamiltonian and k_B is the Boltzmann's constant. While this method is widely used, particularly for suitably coarse grained models, where many of the atomistic degrees of freedom are disregarded, it does not seem to offer any particular advantage for the atomistic simulation of inorganic glasses. Hence this technique will not be described here either.

Basic Features of a Molecular Dynamics Program: an Introduction for the Novice

The equations of motions that are solved in elementary MD are Newton's equations for N atoms with Cartesian coordinates $\{\vec{r}_i\}$, $i = 1, \ldots, N$, ∇_i being the gradient operator with respect to $\vec{r}_i$,

$$m_i\ddot{\vec{r}}_i = -\nabla_i U \equiv \vec{f}_i, \quad \vec{v}_i \equiv \dot{\vec{r}}_i = d\vec{r}_i/dt, \tag{1}$$

where m_i is the mass of particle i and $\vec{f}_i$ is the force on atom i, derived from the potential energy function U of the system,

$$U(\vec{r}_1, \vec{r}_2, \ldots, \vec{r}_N) = \sum_{i=1}^{N}\sum_{j>i}^{N} u(|\vec{r}_i - \vec{r}_j|). \tag{2}$$

In Eq.(2) we have made the approximation that U is simply the sum of *pair* potentials between atoms, which clearly will not be true in general, but which greatly simplifies the calculations since then the force $\vec{f}_i$ simply becomes

$$\vec{f}_i = -\sum_{j(\neq i)=1}^{N} \partial u(|\vec{r}_i - \vec{r}_j|)/\partial\vec{r}_i = \sum_{j(\neq i)=1}^{N} \vec{f}_{ij}. \tag{3}$$

In fact, it is not at all obvious that the directional covalent bonds in materials such as SiO_2, B_2O_3 etc. can be reliably modelled by Eq.(2), and indeed potentials are sometimes used that explicitly include three-body terms that keep a bond angle θ close to its equilibrium value θ_0, e.g. [10, 11]

$$u_\theta = \frac{1}{2}K_\theta(\theta - \theta_0)^2. \tag{4}$$

However, while in the case of B_2O_3 even inclusion of terms such as Eq.(4) still does not allow a fully satisfactory modelling of glassy structures [11], in the case of SiO_2 the situation seems to be fortunately much simpler, and a pairwise potential proposed by *van Beest et al.* [12], henceforth referred to as "BKS potential", already gives reliable results [6,13,14]. With the abbreviation $r_{ij} = |\vec{r}_i - \vec{r}_j|$, the BKS potential is given by

$$u(r_{ij}) = q_i q_j e^2/r_{ij} + A_{ij}\exp(-B_{ij}r_{ij}) - C_{ij}r_{ij}^{-6} \quad \text{with} \quad i,j \in \{\text{Si,O}\}. \tag{5}$$

Here e is the charge of an electron. Note that q_{O} and q_{Si} are *effective charges*, i.e. are given by -1.2 and 2.4, respectively ($q_{\text{Si}} + 2q_{\text{O}} = 0$ is required because of charge neutrality, of course). Apart from this (pseudo-) Coulomb interaction between every pairs of atoms, the only short range interactions present are the ones between Si–O pairs and O–O pairs, with parameters $A_{\text{OO}} \approx 1389$ eV, $A_{\text{SiO}} \approx 18004$ eV, $B_{\text{OO}} \approx 2.76$ Å^{-1}, $B_{\text{SiO}} \approx 4.873$ Å^{-1}, and $C_{\text{OO}} = 175$ eVÅ^{-6}, $C_{\text{SiO}} \approx 133.6$ eVÅ^{-6} [3.12].

As is well-known, Newton's equations conserve the total energy $E = U + K$, where K is the kinetic energy,

$$K = \sum_{i=1}^{N} \frac{1}{2} m_i \left(\dot{\vec{r}}_i\right)^2 . \tag{6}$$

If one solves these equations numerically for a (closed) system of N atoms in a box of volume V, one generates a trajectory through phase space from which one can compute the time average of various physical observables. Since E, N, V are fixed one therefore realizes the microcanonical ensemble of statistical mechanics. Since we deal with classical statistical mechanics, temperature T can be inferred from the equipartition theorem and thus, if the system is in thermal equilibrium throughout the MD "run", we have

$$\overline{K} = 3Nk_BT/2. \tag{7}$$

(By a bar we henceforth denote the time average along the trajectory.) Similarly, pressure can be computed from the virial theorem

$$p = \frac{1}{V}\left\{Nk_BT + (1/3)\sum_{i=1}^{N}\overline{\vec{r}_i \cdot \vec{f}_i}\right\}. \tag{8}$$

In statistical mechanics, one often wishes to use an ensemble where V and T or p and T rather than V and E are the given independent variables. While in the thermodynamic

limit these various ensembles yield equivalent results, for finite N systematic differences occur. Furthermore it is also important to note that any time average $\overline{A}$ can be estimated only to within a certain "statistical error", because of the finite time span covered by the MD run. Thus generalizations of MD for the microcanonical ensemble to these other ensembles are useful and widely used (in "constant pressure" MD one needs to couple the system to a piston, in "constant temperature" MD to a thermostat, etc. [4]). For derivations and details about these extensions, we refer to the literature [4]. Here we only mention another aspect related to the finite size of the simulated system, and this is the aspect of boundary conditions on the surface of the simulation box (which for fluids and amorphous systems usually is taken of cubic shape, $V = L^3$, where L is the linear dimension of the box). Since one is typically interested in bulk behavior of the simulated material, and one wishes to work with only about 10^3 to 10^4 atoms due to limited computer resources, it is crucial to make disturbances due to these boundaries as small as possible. This is achieved by using periodic boundary condition, i.e. the box is surrounded by identical images of itself centered at all integer multiples of L (when the center of the original box is taken as the origin of the coordinate system) and thus the system becomes quasi-infinite. Of course, only the particles in the central box are independent and need to be handled by Newton's equations, but if a particle leaves the box through, say, the surface on its right, the next image of that particle enters the box from the left. While these surfaces thus have no physical effects whatsoever, i.e. surface effects are completely eliminated, it is important to realize that effects associated with the finiteness of N are still present. With respect to thermodynamic properties, such finite size effects are well known (e.g. "rounding" of phase transitions [9]), but one must also be aware that the dynamics of the system may be affected as well (e.g. a phonon mode traveling to the right may re-enter the box from the left and interfere with itself, etc. [15]).

The periodic boundary condition must also be correctly treated when one considers interactions among distant particles. For slowly decaying potentials, such as the Coulomb part in Eq.(5), it is essential to sum the interactions not only over all particles in the

primary box but also over all the periodic images — every atom interacts thus with an infinite number of images of all the other particles! This seemingly difficult task, however, is efficiently solved by the Ewald method [4]. For the short range part, however, one may even follow the simpler strategy to cut the potential off if the distance r exceeds a maximum distance $r_{\max}$ (e.g., for the O–O-interaction in [6] $r_{\max} = 5.5$ Å could be used since then the strength of the potential has decreased to about 1 % of its value at the preferred O–O distance).

As a last point, we emphasize that integration of Newton's equations, Eq.(1), for a many-particle system of interest cannot be done exactly, but only approximately, due to the finiteness of the time step δt of the numerical integration procedure. By making δt sufficiently small this error can be made as small as desired — but then it becomes increasingly difficult to propagate in time up to time scales of physical interest. Thus it is important to choose a "good" integration algorithm. Several suitable algorithms exist, but here only the standard Verlet algorithm is quoted [4], which is correct up to order $(\delta t)^3$,

$$\vec{r}_i(t+\delta t) = \vec{r}_i(t) + \delta t \vec{v}_i(t) + \frac{1}{2m_i}(\delta t)^2 \vec{f}_i(t), \tag{9}$$

$$\vec{v}_i(t+\delta t) = \vec{v}_i(t) + \frac{\delta t}{2m_i}[\vec{f}_i(t) + \vec{f}_i(t+\delta t)]. \tag{10}$$

Note that the propagation of the velocities, Eq.(10), requires that the forces are known both at the present time t and at the next time step $t+\delta t$, which can of course be calculated from $\vec{r}_i(t+\delta t)$ using Eq.(3). This algorithm is time reversible and conserves the phase space volume of a continuous set of phase space points, as is required for time averaging in statistical mechanics [4]. Nevertheless, it is clearly necessary that δt is at least about two orders of magnitude smaller than the time constant of elementary physical motions in the system, e.g. vibration times of covalent Si–O-bonds or bond angles, which are significantly less than one pico second: Therefore it becomes necessary to choose a time-step δt as small as $\delta t = 1.6 \times 10^{-15}$ sec to get reliable results! Thus even very long MD runs (several millions of time steps) can span only a very short interval of physical time, of the order of 10 nano sec. This is not only true for SiO_2 but for MD simulations of atomistic models of real materials in general. While experimental techniques such as neutron scattering

[16] are constrained to a similarly restricted "observation time window", the important distinction is that in MD the same short time scale is available not only for observation but also for the *equilibration of the structure*. Therefore the way how a structure for an amorphous material studied by MD was prepared needs careful attention — although this is an obvious point, it often is "swept under the rug" in the literature!

For example in the results described in the next section, this "preparation of the system" was done by making first an MD run of 40,000 time steps at an initial temperature $T_i = 7000K$. This length is more than enough to equilibrate the system at this extremely high temperature. Subsequently the system was cooled, at zero pressure, by coupling it to a heat bath whose temperature $T_b(t)$ was decreased linearly in time, $T_b(t) = T_i - \gamma t$, with cooling rates γ from 1.14×10^{15} K/s to 4.44×10^{12} K/s. Even the slowest cooling rate is many orders of magnitude larger than the ones used in the laboratory. However, it is currently not possible to simulate a quench of the system with cooling rates that are significantly smaller than the ones used here, since for the smallest cooling rate one simulation run of the system (which contained 334 Si- and 668 O-atoms in the central box) needs already about 340 h of CPU time on an IBM RS6000/370 workstation, and one needs to take a sample average over at least 10 independent runs (starting from different initial configurations) to improve the statistical accuracy of the "simulation data".

A Case Study: Cooling-Rate Dependence of the Structure of amorphous SiO_2

Here we briefly review some typical results that were recently obtained by *Vollmayr et al.* [6]. As an example for macroscopic properties we show in Fig. 1 the temperature dependence of the density for the different cooling rates studied. One sees that, at very high temperatures, all curves (apart from the ones for the three fastest cooling rates) fall onto a master curve, the equilibrium curve. However, for the fastest cooling rates the system falls out of equilibrium during the cooling process immediately, demonstrating that even at extremely high temperatures such runs do not give any reliable information on the thermal equilibrium behavior of the system.

The curves corresponding to the smallest cooling rates show a maximum at around

4800 K, i.e. a density anomaly. Qualitatively, but not quantitatively, this anomaly is in agreement with experiment (the experimental value for the temperature of the density maximum is considerably lower, namely 1820 K [17]). It is unlikely that this quantitative discrepancy is related to the too fast cooling since the location of the maximum is independent of the cooling rate, if the latter is sufficiently small. More probably the discrepancy reflects an inaccuracy of the potential. However, for different potentials this density anomaly is present only at even higher temperatures or not present at all [18]: thus nothing would be gained by using instead of Eq.(5) one of these (typically more complicated) alternative potentials.

For intermediate and small values of γ, the density decreases upon cooling (after having passed the maximum) and reaches a minimum. At even lower temperatures the curves become, within the accuracy of our data, straight lines with negative slope. The value of this (positive) thermal volume expansion coefficient α decreases with decreasing cooling rate from about $\alpha_p \approx 7 \times 10^{-6}$ K^{-1} for $\gamma = 1.14 \times 10^{15}$ K/s to $\alpha_p \approx 2.5 \times 10^{-6}$ K^{-1} for $\gamma = 4.44 \times 10^{15}$ K/s. Experimental values at and above room temperature are [17] $\alpha_p \approx 0.55 \times 10^{-6}$ K^{-1}. Note, however, that quantum statistical mechanics requires that $\alpha_p(T \to 0) \to 0$, i.e. the density must reach its groundstate value with vanishing slope. This feature can never be reproduced by a purely classical calculation such as MD. In fact deviations from classical statistical mechanics are expected at temperatures of the order of the Debye temperature, which is roughly $T_\Theta \approx 1200$ K in SiO_2 [19]. A similar caveat also applies to the specific heat C_p, which reaches in the MD simulation [6] at low temperatures a value of about 1.25 J/gK, close to the value of the classical Dulong-Petit law (which would yield 1.236 J/gK): classical MD (as well as classical Monte Carlo) can never reproduce the vanishing of the specific heat as $T \to 0$. (In principle, this can be achieved by the quantum-mechanical path integral Monte Carlo method [3] but this approach has so far only been applied to crystals and not yet to glasses.)

While experimentally [19] C_p rises rather sharply at the glass transition temperature from about 1.23 J/gK to about 1.5 J/gK, the simulation yields a smooth increase at about $T = 3000$ K to a maximum value of $C_p^{\max} \approx 2$ J/gK near $T = 4000$ K; the latter behavior

is thus not backed by experiment and may partially be due to artifacts of the too rapid cooling and partially due to inadequacies of the potential [5].

Although the MD simulation of molten SiO_2 using the BKS potential gives neither at very high temperatures nor at low temperatures a *quantitatively* accurate description of thermal properties (density, specific heat, etc.), it nevertheless gives a very good description of the geometric structure of the glass. This is evident if one examines the radial distribution functions $g_{\alpha\beta}(r)$ between species α and β, Fig. 2 (see Ref. [20] for theoretical background on this quantity). One recognizes that with decreasing cooling rate the structural order at short and intermediate distances (i.e. $r \leq 8$ Å) increases, since the peaks and minima of $g_{\alpha\beta}(r)$ become more pronounced. The height of the first-nearest-neighbor peak changes by about 20 %! The amount of this change is significantly larger than any change observed for macroscopic properties [6] and thus we conclude that microscopic properties can show a much stronger dependence on the cooling rate than the macroscopic properties do.

From Fig. 2 one also sees that although the *height* of the various peaks shows a significant cooling-rate dependence, the *location* of the peaks is affected much less by the variation of γ. Thus it is reasonable to compare these positions with experimental data, indicated in broken lines. E.g., Mozzi and Warren [21] quoted for the location of the 1^{st} and 2^{nd} peak 1.62, 4.15; 2.65, 4.95; 3.12, 5.18 Å for SiO, OO and SiSi, respectively. Although the agreement is not perfect, the BKS potential does quite well to reproduce the short and medium-range order of silica glass. Note that this potential was developed to describe the *crystalline* modifications of SiO_2, and in Ref. [6] it was used for amorphous SiO_2 without adjusting any parameter whatsoever.

Similar conclusions emerge from a discussion of the partial structure factors $S_{\alpha\beta}(q)$ [6], where q is the scattering wavenumber, which is the structural quantity that is most directly accessible in diffraction experiments. But the advantages of the simulation is that full microscopic details of the structure are much more easily accessible. Since Fig. 2 shows that the location $r_{\min}$ of the first minimum in the radial distribution function is practically independent of γ (namely $r_{\min}^{\mathrm{SiSi}} = 3.42$ Å, $r_{\min}^{\mathrm{SiO}} = 2.20$ Å, and $r_{\min}^{\mathrm{OO}} = 3.00$ Å),

one can compute unambiguously the (partial) coordination number z of particle i by defining z as the number of other particles j with $|\vec{r}_j - \vec{r}_i| < r_{\min}$. Fig. 3 shows $P_{\alpha\beta}^{z=n}$, the probability that a particle of type α has n nearest neighbors of type β. The vast majority of silicon atoms are surrounded by $z = 4$ oxygens; the case $z = 5$ occurs for the fast cooling rate with probability 5 % and decreases to about 0.5 % probability for the slowest cooling rate. Similarly $z = 2$ dominates for oxygens. Thus the BKS potential automatically yields the "rules" commonly postulated for ideal amorphous SiO_2, namely that this system is a "continuous random network" with these coordination numbers $z = 4$ for Si and $z = 2$ for O [8].

More disorder, however, is found on an intermediate length scale: while each SiO_4 tetrahedron is surrounded by four other tetrahedra on average, even for the smallest cooling rate the probability $P_{\mathrm{SiSi}}^{z=5}$ is still about 1.5%, and $P_{\mathrm{OO}}^{z=6}$ increases only from about 0.6 to 0.87 with decreasing cooling rate, over the accessible range of γ (about 10% of the oxygen atoms have seven other oxygen atoms as second nearest neighbors instead of six). The spread in these next-nearest neighbor coordinations in the network is a clear indication of disorder.

This disorder also shows up clearly in the distribution functions of various bond angles (Fig. 4). It is remarkable that the distribution $P_{\mathrm{OSiO}}(\theta)$ has its maximum at an angle close to the value of an ideal tetrahedron (109.47°), and that the width of this distribution clearly narrows with decreasing cooling rate. As far as experimental data on the peak positions of these angular distributions and their halfwidths are available at all, the simulations for the slowest cooling rate are already very close to the experimental values. This shows that such simulations can give quite reliable information on such quantities.

Another characteristic of the medium range order in glasses, that is much discussed in the literature, is the distribution of the frequency of *rings* of a given size. A ring is defined as follows: starting from a Si atom one chooses two different O atoms that are nearest neighbors. Pick one of these. In general this O atom will also be a nearest neighbor of a second Si atom. From this new Si atom one then picks a new nearest-neighbor O atom, etc. This process is continued until one returns to the O atom which is the second one

of the nearest-neighbor O atoms of the first Si-atom. In this way one has constructed a closed loop of Si–O segments. The shortest one of these loops is called the ring associated with the original Si atom and the two nearest-neighbor O-atoms. The number of Si–O segments in this loop is called the size n of this ring.

Fig. 5 shows $P(n)$, the probability that a ring has length n, as function of the cooling rate. As expected, the case $n = 6$ dominates, and $P(n)$ for small n ($n = 3, 4$) clearly decrease with decreasing γ. Note that in β-cristobalite (the first crystalline phase reached from the liquid) only $n = 6$ occurs, while the lower-temperature phases β-tridymite and β-quartz have rings with both $n = 6$ and $n = 8$, but no odd-numbered rings. The large numbers of rings with $n = 5$ and $n = 7$ can be considered as a hallmark of amorphous silica, and the difficulty to eliminate these "defects" from the structure prevents the system to crystallize easily.

Concluding remarks

In the previous subsection, it was demonstrated (choosing the work [6] as an example) that with the slowest cooling rates just available, it is now possible to create "good" amorphous silica structures, which agree surprisingly well with experimental findings, despite the fact that the simulated cooling rate exceeds the experimental one by many orders of magnitude. However, clear discrepancies remain when one considers the temperature dependence of various quantities, because first of all the system falls out of equilibrium at a much higher temperature than in the experiment, and secondly because quantum effects are missing and they are expected to become increasingly important at low temperatures. Of course, we expect that, if the length scales we consider increase, we will find a stronger dependence of the medium range order on the cooling rates, some evidence in this direction was already discussed here, and the more the simulated model will differ from reality (since quantitative information on properties like the ring statistics, Fig. 5, is not available from experiment, this expected discrepancy is not yet detectable in practice: pair correlations $g_{\alpha\beta}(r)$ or structure factors $S_{\alpha\beta}(q)$ simply are too insensitive probes of amorphous structures!).

Nevertheless, the rich information from the MD simulation on a large variety of structural properties $\{g_{\alpha\beta}(r)$, partial coordination numbers, bond angle distributions, ring statistics, etc.$\}$, and the dependence of these properties on both temperature and cooling rate, allows to correlate these properties with each other and thus to gain insight into how and why the amorphous structure forms. We feel that this insight still may be partially unraveled, and additional studies are desirable (including studies with other potentials that have been used in the literature).

One major challenge, of course, is the extension of these studies from pure SiO_2 to silicate glasses that contain more components. One obvious obstacle to simulate, say, a mixture of SiO_2 and B_2O_3 is that presently the interaction of a pair of oxygen in SiO_2 is modelled by a completely different function [12] than in B_2O_3 [10,11]. But promising first steps to model more-component glasses such as sodium silicate glasses have been taken a long time ago [22], and we think time is ripe to resume such efforts.

Acknowledgements:

This brief review is largely based on research done jointly with K. Vollmayr {Ref.[6]}. It is a great pleasure to thank her for a very pleasant and fruitful collaboration. We also have significantly profited from collaborations with H.C. Andersen, C.A. Angell, J. Horbach, J.L. Barrat, and others. Stimulating and informative discussions with U. Buchenau, U. Fotheringham, D. Krause, W. Pannhorst and R. Sprengard also deserve mention. Last but not least we thank the SCHOTT Glaswerke Fonds and the Deutsche Forschungsgemeinschaft (DFG, grant No. SFB 262/D1) and the Bundesministerium für Bildung, Forschung, Wissenschaft und Technologie (BMBF, grant No. 03N8008C) for financial support for this research.

References

1 W. Kohn: "Density functional theory", in *Monte Carlo and Molecular Dynamics of Condensed Matter Systems*, ed. by K. Binder, G. Ciccotti (Societá Italiana di Fisica, Bologna, 1996) pp. 561-572

2 R. Car: "Molecular dynamics from first principles", in *Monte Carlo and Molecular Dynamics of Condensed Matter Systems*, ed. by K. Binder, G. Ciccotti (Societá Italiana di Fisica, Bologna, 1996) pp. 601-634

3 P. Nielaba: "Quantum simulations in materials science: Molecular monolayers and crystals", in *Annual Reviews of Computational Physics V*, ed. by D. Stauffer (World Scientific, Singapore, 1997) pp. 137-199

4 M. Sprik: "Introduction to molecular dynamics methods", in *Monte Carlo and Molecular Dynamics of Condensed Matter Systems*, ed. by K. Binder, G. Ciccotti (Societá Italiana di Fisica, Bologna, 1996) pp. 43-88

5 C. A. Angell, J. H. R. Clarke, L. V. Woodcock: "Interaction potentials and glass formation: a survey of computer experiments", in *Advances in Chemical Physics*, Vol. XLVIII, ed. by I. Prigogine, S. Rice (J. Wiley, New York, 1981) pp. 397-453

6 K. Vollmayr, W. Kob, K. Binder: "Cooling-rate effects in amorphous silica: A computer simulation study" Phys. Rev. B **54**, 15808-15827 (1996)

7 W. Kob: "Computer Simulations of Supercooled Liquids and Structural Glasses", in *Annual Reviews of Computational Physics III*, ed. by D. Stauffer (World Scientific, Singapore, 1995), pp. 1-43

8 R. Zallen: "Stochastic geometry: Aspects of amorphous solids", in *Fluctuation Phenomena*, ed. by E. W. Montroll, J. L. Lebowitz (North-Holland, Amsterdam, 1979), pp. 177-228

9 K. Binder: "Applications of Monte Carlo Methods to Statistical Physics" Rep. Progr. Phys. **60**, 487-559 (1997)

10 A. Takada, C. R. A. Catlow, G. D. Price: "Computer modelling of B_2O_3: part I. New interatomic potentials, crystalline phases, and predicted polymorphs" J. Phys.: Cond. Matter **7**, 8659-8692 (1995)

11 A. Takada, C. A. R. Catlow, G. D. Price: "Computer modelling of B_2O_3: part II. Molecular dynamics simulations of vitreous structures" J. Phys.: Cond. Matter **7**, 8693-8722 (1995)

12 B. W. H. van Beest, G. J. Kramer, R. A. van Santen: "Force fields for silicas and aluminophosphates based on *ab initio* calculations", Phys. Rev. Lett. **64**, 1955-1958 (1990)

13 J. Horbach, W. Kob, K. Binder: "Molecular dynamics simulations of the dynamics of supercooled silica", Phil. Mag. B (in press)

14 J. Horbach, W. Kob, K. Binder: "The dynamics of supercooled silica: acoustic modes and boson peak", J. Non-Cryst. Solids (in press)

15 J. Horbach, W. Kob, K. Binder, C. A. Angell: "Finite size effects in simulations of glass dynamics", Phys. Rev. E **54**, R5897-R5900 (1996)

16 U. Buchenau: "Neutron scattering at the glass transition", in *Phase Transitions and Relaxation in Systems with Competing Energy Scales*, ed. by T. Riste and D. Sherrington (Kluwer Acad. Publ., Dordrecht, 1993) pp. 233-257

17 O. V. Mazurin, M. V. Streltsina, T. P. Shvaikoskaya: *Handbook of Glass Data* (Elsevier, Amsterdam, 1983) Part A

18 B. Vessal, M. Amini, D. Fincham, C. R. A. Catlow: "Water-like melting behavior of SiO_2 investigated by the molecular dynamics simulation technique", Phil. Mag. B **60**, 753-775 (1989)

19 R. Brückner: "Properties and Structure of Vitreous Silica. I" J. Non-Cryst. Solids **5**, 123-175 (1970)

20 J.-P. Hansen, I.R. McDonald: *Theory of Simple Liquids* (Academic, London, 1986)

21 R. L. Mozzi, B. E. Warren: "The Structure of Vitreous Silica" J. Appl. Cryst. **2**, 164-172 (1969)

22 T. F. Soules "A molecular dynamics calculation of the structure of sodium silicate glasses", J. Chem. Phys. **71**, 4570-4578 (1979)

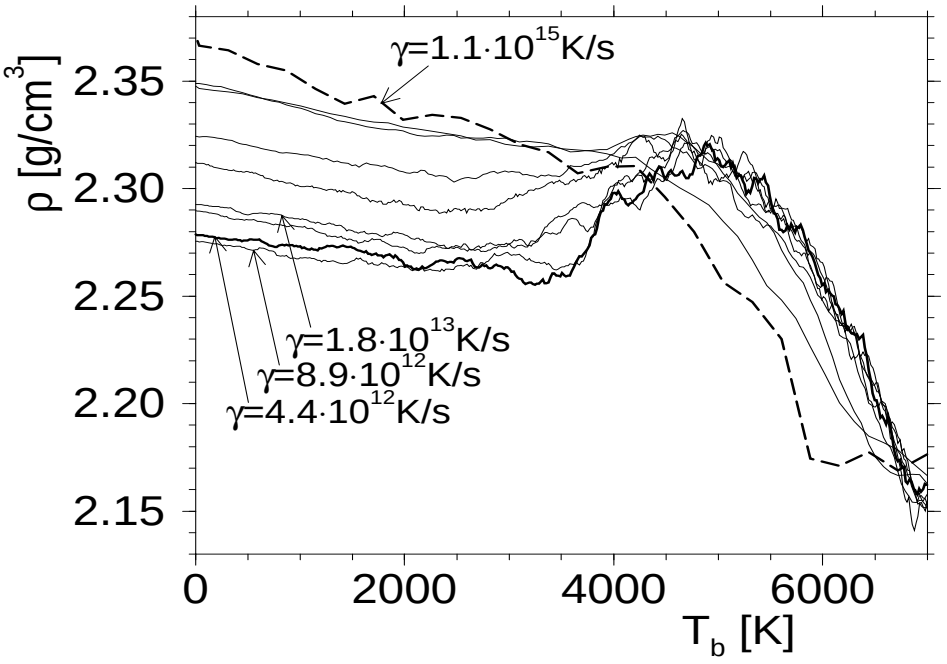

Figure 1: Density of simulated SiO_2 vs. bath temperature T_b, for all cooling rates investigated. The solid and dashed bold curves are the smallest and largest cooling rates γ, respectively. Note the presence of a local maximum in ρ at temperatures around 4800 K if γ is small. From *Vollmayr et al.* [6].

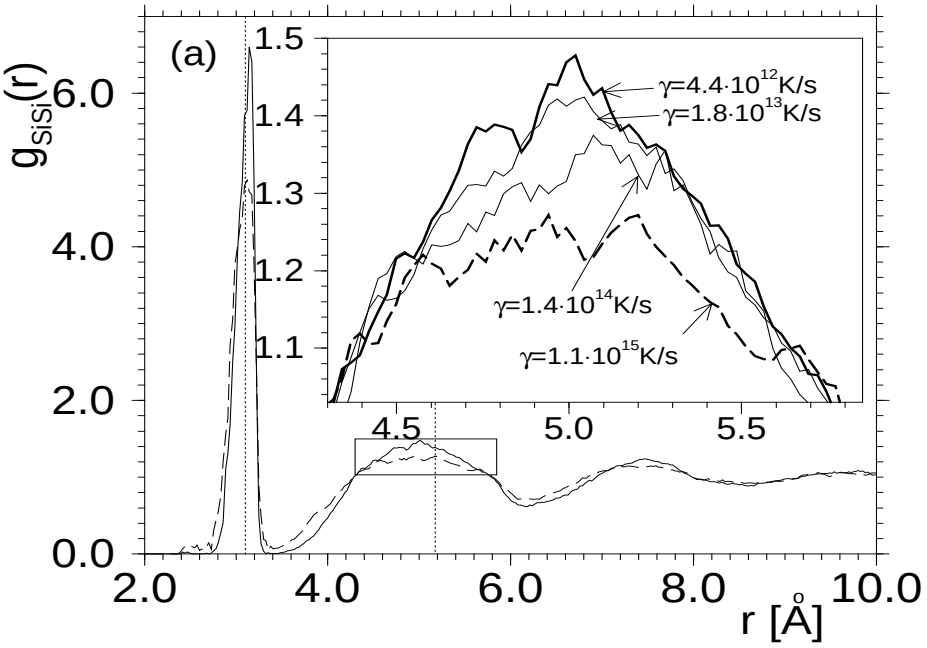

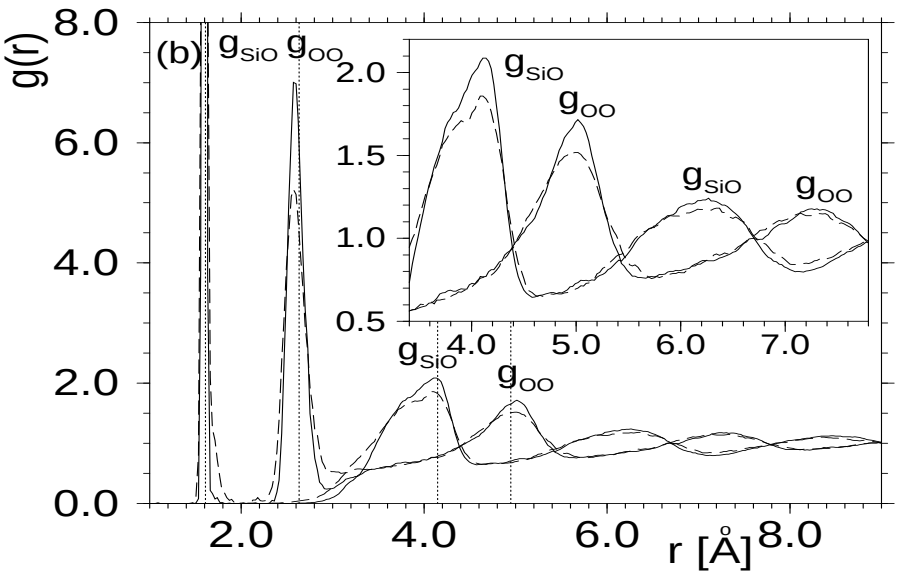

Figure 2: Radial distribution functions of simulated amorphous SiO_2. (a) $g_{\mathrm{SiSi}}(r)$. Main figure: the slowest (solid curve) and fastest (dashed curve) cooling rate. The vertical dotted lines give the position of the peak as determined from experiments (see text). Inset: enlargement of the second-nearest neighbor peak for four selected cooling rates. (b) $g_{\mathrm{SiO}}(r)$ and $g_{\mathrm{OO}}(r)$ for the slowest (solid curves) and fastest (dashed curves) cooling rate. Inset: enlargement of the second-and third-nearest-neighbor peak. From *Vollmayr et al.* [6].

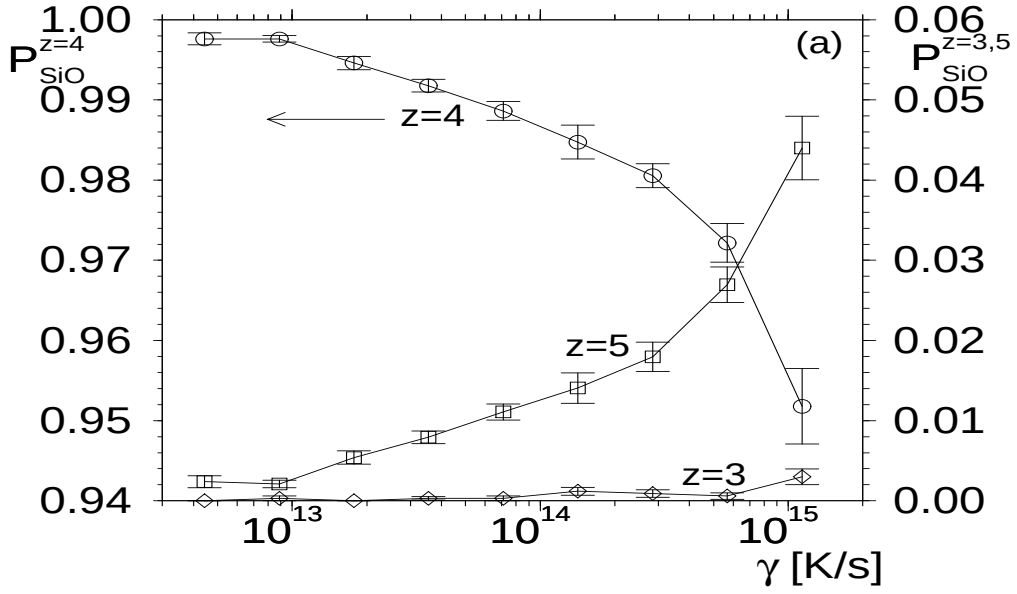

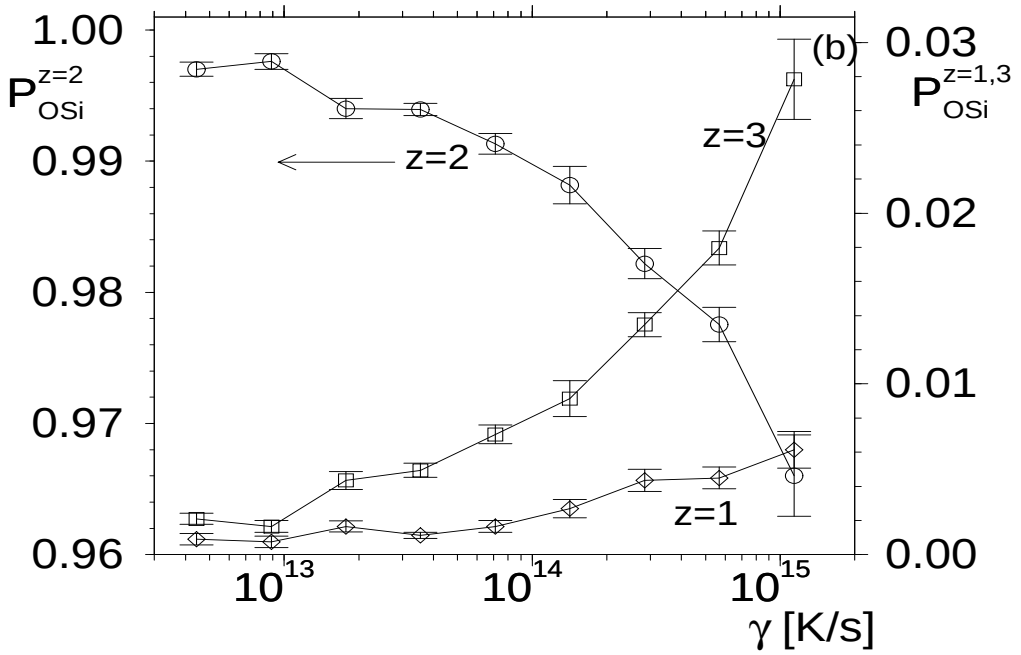

Figure 3: Probabilities of partial coordination numbers $P_{\alpha\beta}^{z=n}$ plotted vs. cooling rate, for Si–O pairs (a) and O–Si pairs (b). Note the different scales for the various curves. From *Vollmayr et al.* [6].

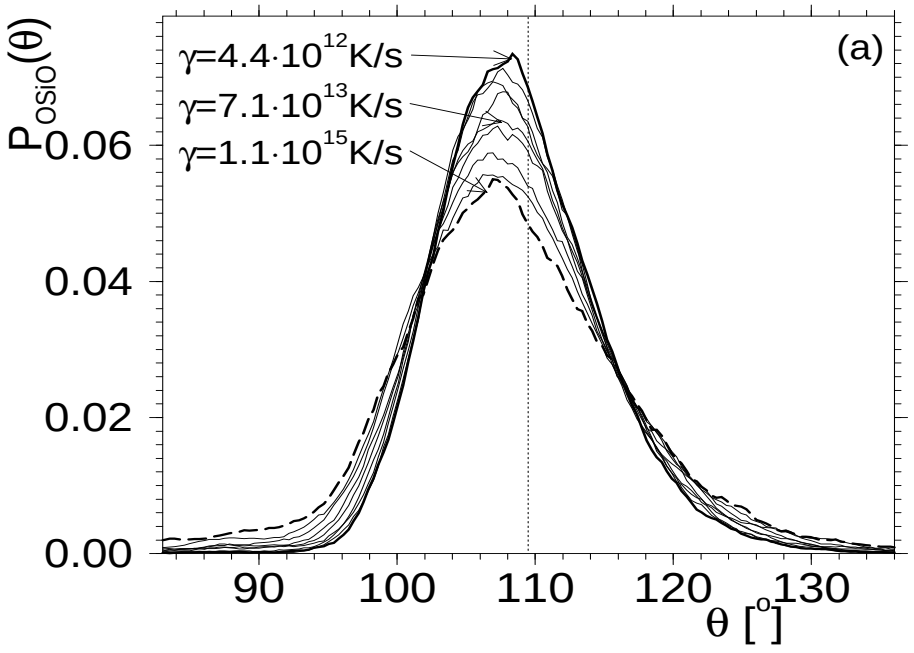

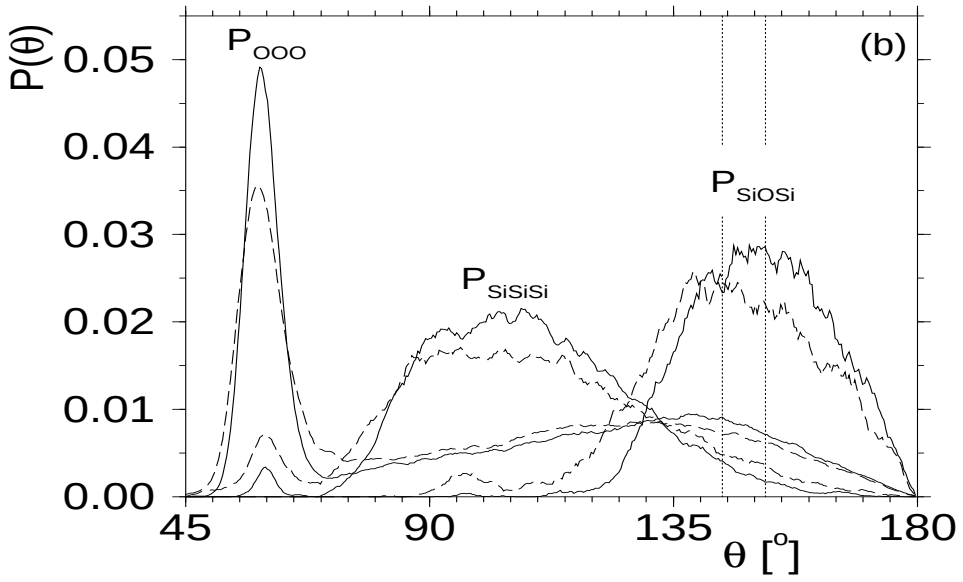

Figure 4: Distribution function of various angles at several cooling rates in amorphous SiO_2 at $T = 0$. (a) Angle O-Si-O for all cooling rates studied. The vertical line is the experimental value [21]. (b) Angles O-O-O, Si-Si-Si and Si-O-Si for the slowest (solid curves) and fastest (dashed curves) cooling rates investigated. Vertical lines are experimental values from different authors (see [6] for details.). From *Vollmayr et al.* [6].

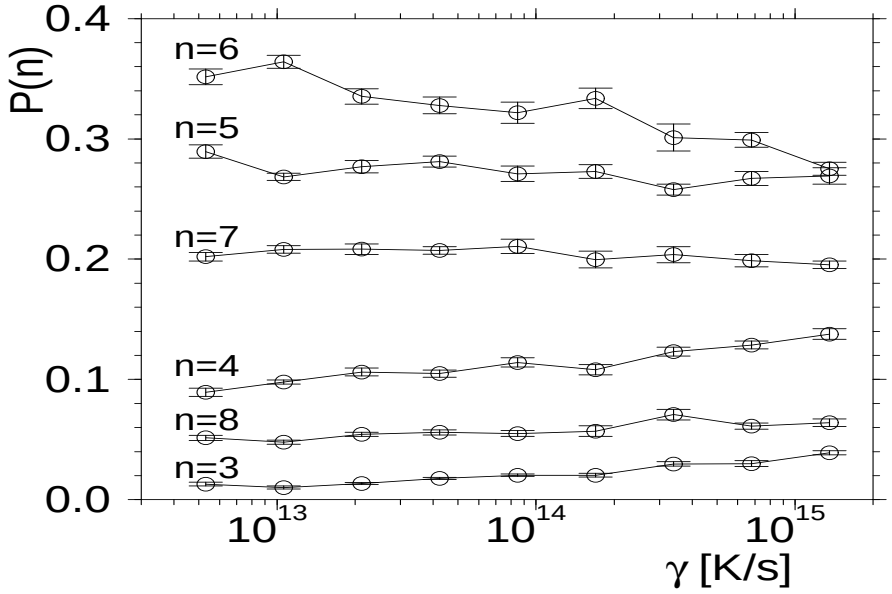

Figure 5: Probability $P(n)$ that a particle is a member of a ring of size n, plotted vs. γ. From *Vollmayr et al.* [6].